Astron. Astrophys. 348, 627–635 (1999)

ASTRONOMY AND ASTROPHYSICS

Power spectra comparison between GOLF and spatially masked MDI velocity signals

C.J. Henney[1], R.K. Ulrich[1], L. Bertello[1], R.S. Bogart[2], R.I. Bush[2], P.H. Scherrer[2], T. Roca Cortés[3], and S. Turck-Chièze[4]

[1] Department of Physics and Astronomy, UCLA, Los Angeles, CA 90095-1562, USA
[2] Stanford University, CSSA-HEPL, Stanford, CA 94305-4085, USA
[3] Instituto de Astrofísica de Canarias, Departamento de Astrofísica, U. de La Laguna, E-38200 La Laguna, Spain
[4] Service d'Astrophysique, DSM/DAPNIA, CE Saclay, F-91191 Gif-sur-Yvette, France

Received 19 April 1999 / Accepted 9 June 1999

Abstract. The Global Oscillations at Low Frequency (GOLF) and the Michelson Doppler Imager (MDI) instruments aboard the Solar and Heliospheric Observatory (SOHO) give an excellent opportunity to search for solar low frequency oscillation modes previously undetected from ground based experiments. Presented here is a comparison of the velocity power spectra between the two instruments. In addition, this paper outlines work towards creating a GOLF-simulated signal utilizing MDI velocity images. The simulation of the GOLF signal is achieved by integrating spatially weighted masks with MDI full-disk Doppler images. The GOLF-simulated signal and a selection of additional spatially masked MDI velocity signals are compared with the observed GOLF signal for a 759 day period from May 25, 1996 through June 22, 1998. Ultimately, a cross-analysis process between GOLF and MDI signals could lead to an enhancement of our ability to detect low frequency solar oscillations. For low degree ($l \leq 3$) and low frequency acoustic modes, the signal-to-background ratio between GOLF and the spatially masked MDI velocity data is compared here.

Key words: Sun: atmosphere – Sun: oscillations

1. Introduction

Instrument details and project goals of the Global Oscillations at Low Frequency (GOLF) and the Michelson Doppler Imager (MDI) instruments aboard the Solar and Heliospheric Observatory (SOHO) are outlined in Gabriel et al. (1995) and Scherrer et al. (1995) respectively. Preliminary results from GOLF are presented by Gabriel et al. (1997) and Turck-Chièze et al. (1997). Additionally, initial results from the MDI instrument are presented by Kosovichev et al. (1997) and Duvall et al. (1997). One of the mission objectives of both the GOLF and the MDI instruments on SOHO is the detection of new low frequency globally coherent oscillation modes. After more than two years of nearly continuous observation of the sun by both instruments, the clear detection of modes below 1000 μHz has still proven to be elusive. The search for new modes may be aided by combining the high coverage of GOLF with the spatial resolution and various data products of MDI. By combining the two data sets, a signal enhancement is anticipated since both instruments provide a low noise data stream and their sources of solar and instrumental noise are expected to be different from each other.

The GOLF and MDI instruments differ in many respects. For the period investigated here, the GOLF instrument measured the intensity of the integrated solar disc on the blue wing of the doublet Na D lines. The MDI instrument utilizes a mid-photospheric absorption line, Ni I 676.8nm, and it is designed to measure the intensity at five positions on or near the line profile using a pair of tunable Michelson interferometers. These differences cause the two instruments to respond to solar phenomena with differing sensitivity. For example the sodium lines are formed near the temperature minimum where acoustic modes may have a larger amplitude due to the solar atmospheric density gradient. Supergranulation is mostly confined to the photospheric layers and may contribute less incoherent velocity variation to an instrument like GOLF deriving its signal from the temperature minimum.

Ideally we want to synthesize a GOLF-simulated velocity signal from the spatially resolved MDI velocity images and compare that directly to the observed GOLF signal. A GOLF-simulated signal may be useful in comparing the instrumental performances of both GOLF and MDI. Since the GOLF instrument is sensitive to solar magnetic activity, the MDI magnetic proxy data may be functional in removing active region effects from the observed GOLF signal (e.g. Ulrich et al. 1993). Correspondingly, the sodium cell design of the GOLF instrument allows for an atomic wavelength reference, whereas the MDI instrument relies on a thermal system to remain optically stable. Thus, both data sets may be beneficial to each other in terms of calibration.

Previous MDI and GOLF velocity signal comparisons showed excellent agreement in the 5-minute band (e.g. Toutain et al. 1997, Henney et al. 1998a and Pallé et al. 1999). In the range 1300 to 4000 μHz, the low degree ($l \leq 3$) acoustic mode frequency differences between the two instruments are found to be within the error of the measurements (Toutain et al. 1997

Send offprint requests to: C.J. Henney
Correspondence to: henney@astro.ucla.edu

and Bertello et al. 1998). In addition, a GOLF-simulated velocity signal similar to the one presented in this paper showed a slight improvement in the correlation with the GOLF signal relative to the `raw´ integrated full-disk MDI velocity signal (Henney et al. 1998a).

In the following sections the procedure used to create the MDI masked velocity signals is outlined, along with power spectra comparison between MDI and GOLF signals. The observed GOLF signal and the modeled GOLF velocity response is discussed in Sect. 2. Signal processing and spatial masking of MDI images is described in Sect. 3. The signal-to-background ratios for low frequency acoustic modes of the MDI and GOLF signals are presented and discussed in Sect. 4.

2. The GOLF signal

The GOLF instrument is a sodium resonant scattering spectrophotometer which measures the integrated photometric signal of the solar disc on either the blue or red wing of the Na D lines. The GOLF sodium cell is positioned in a 5040 ± 40 gauss magnetic field with an additional magnetic field modulation of 76.9 ± 1 gauss from an electromagnet (Ulrich et al. 1998). This allows two photometric measurements on one wing of the Na D line profiles. The signal variation observed by GOLF is primarily a result of velocity and only 15% of the signal in the 5-minute band can be attributed to an intensity-like signal (e.g. Pallé et al. 1999). Due to a malfunction of the rotating mechanism for the linear polarizer and the quarter wave plate, the GOLF instrument observed in the blue wings of the Na D lines for the period investigated here.

The GOLF signal used in this work is an average of the four calibrated velocities using the S method (Ulrich et al. 1998). This calibration method is based on an accurate velocity scaling over the period data acquisition. Four signals are observed since GOLF measures the intensity from two magnetic modulations with two photometers. The four calibrated GOLF signals are filtered using a non-recursive digital filter with a band pass between 30 and 8100 μHz and then resampled into the MDI Doppler data time reference with a cadence of 60s. The GOLF signal coverage is approximately 99% for the period studied in this paper.

2.1. The GOLF velocity response

Following the notation of Ulrich et al. (1999), the signals observed by GOLF in the blue wing of the Na D line profiles, $\delta v_b^{\pm}$, can be represented as

$$\delta v_b^{\pm} = W_0 \int_{\rm disc} S_{v,b}^{\pm}\, \delta v\, dA, \tag{1}$$

where

$$W_0 = \left[\int_{disc} dA \right]^{-1}. \tag{2}$$

In the above relations, the solar surface line-of-sight velocity field and a small surface element projected onto the observing plane are represented by δv and dA respectively. The `$\pm$´ superscript indicates the two electromagnet states. The velocity sensitivity, or response, function, $S_{v,b}^{\pm}$, is derived from Na line profiles observed from the Mt. Wilson 150-foot solar tower at different solar center-to-limb positions and is discussed in detail by Ulrich et al. (1999).

The velocity response function is dependent on the observed velocity, which is the sum of the line-of-sight oscillation velocity and the effective offset velocity signal. During the course of a year the sun-SOHO line-of-sight offset velocity signal, which includes the orbital, gravitational and convective shift velocities, ranges between approximately 100 and 1100 m/s. The computed GOLF velocity sensitivity function is defined here as

$$S_{v,b}^{\pm} = \frac{V_{b0}}{\langle I_b^{\pm} \rangle} \frac{\partial I_b^{\pm}}{\partial v}, \tag{3}$$

where v and V_{b0} are the line-of-sight velocity the conversion factor from fractional intensity change to velocity respectively. In Eq. (3), the GOLF observed intensity from the Na D line profiles in the blue wing at a given solar disc position and the average over the disc is represented by $I_b^{\pm}$ and $\langle I_b^{\pm} \rangle$ respectively.

Due to the change in the observed slope along the wings of the Na line profiles the velocity response function is asymmetric across the solar disc and depends on the effective offset velocity signal. This effect is illustrated in Figs. 1 and 2 for three offset velocities. The GOLF instrument is less sensitive to velocities in the solar disc area rotating away from SOHO when the offset velocity signal is greater than 600 m/s (see Fig. 2). In addition to sampling different parts of the wing due to Doppler shifts of the solar line, the Na D_1 line profile shape is observed to vary due to magnetic activity and center-to-limb position (e.g. Ulrich et al. 1993 and Ulrich et al. 1999). Note that the single wing mode of observing is a photometric measurement, thus the signal includes both intensity and velocity fluctuations. In Eq. (1) the effects of magnetic activity and temperature perturbations are ignored for this preliminary work. The details about calculating $S_{v,b}^{\pm}$ are fully developed in Ulrich et al. (1999).

3. Integrated full-disk MDI velocity signal

Using a pair of tunable Michelson interferometers along with a Lyot and a set of fixed filters, the MDI instrument spatially resolves the solar image onto a 1024×1024 CCD camera in narrow bands (9.4 pm) along the Ni I 676.8nm line profile. The velocity data used here is from the calibrated level-1.4 MDI LOI-proxy Doppler images. The `LOI-proxy´ refers to the image binning mask chosen for comparison between MDI and the Luminosity Oscillations Imager (LOI), which is a part of the Variability of solar Irradiance and Gravity Oscillations (VIRGO) instrument aboard SOHO. Aboard SOHO, the MDI processor averages the 1024×1024 full-disk observations into 180 spatial bins. An example of the MDI LOI-proxy mask is shown in Fig. 1 for Doppler data with the large spatial scale gradients removed (also see Hoeksema et al. 1998). Instrument details and project goals of the VIRGO instrument are outlined in Fröhlich et al. (1995). Initial results from VIRGO and VIRGO/LOI are presented by

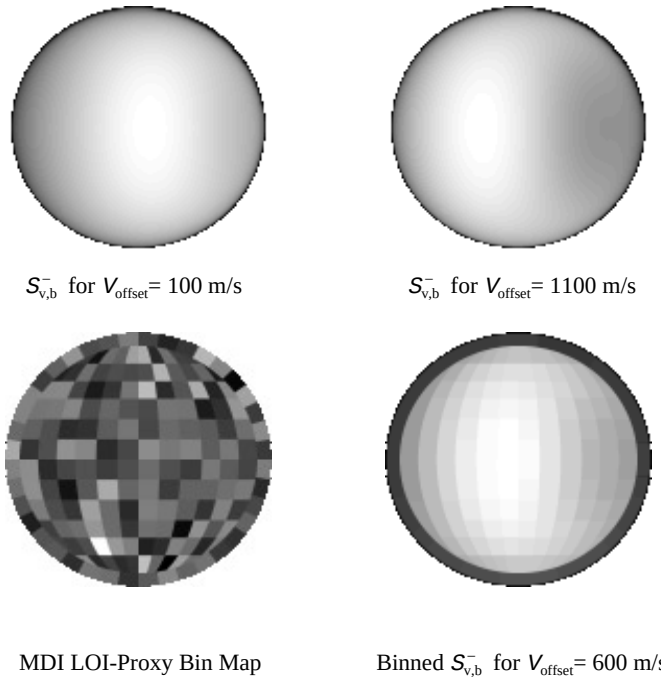

Fig. 1. Examples of the GOLF velocity sensitivity function, $S^-_{v,b}$, illustrating the extremes with the offset velocities of 100 and 1100 m/s (*top row*). Also shown, is an example of a MDI LOI-proxy velocity image with the day average of each bin subtracted to remove large scale spatial gradients (*bottom left*). Binned using the LOI-proxy mask, an example GOLF velocity sensitivity function image for an offset velocity of 600 m/s is shown bottom right. White represents the maximum value and black is the minimum.

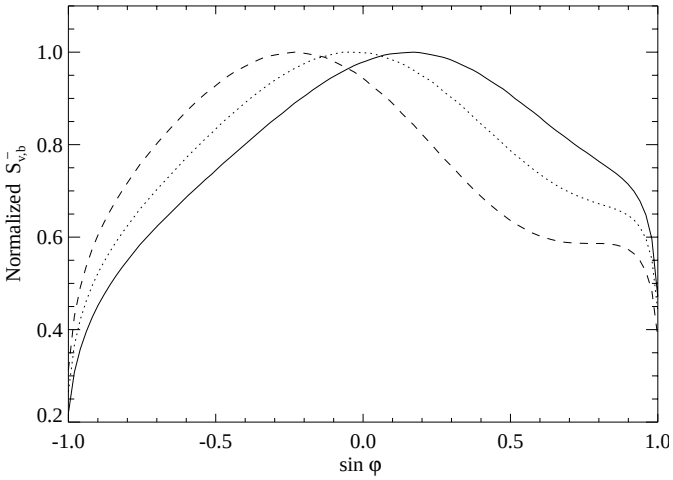

Fig. 2. Example equatorial slices of the GOLF velocity sensitivity function, $S^-_{v,b}$, for effective offset velocities of: 100 m/s (solid), 600 m/s (dot) and 1100 m/s (dash). The central meridian distance angle is represented by φ. The response function slices are normalized by their individual maximum.

Fröhlich et al. (1997) and Appourchaux et al. (1997) respectively.

Temporal gaps in the MDI LOI-proxy data, mostly due to telemetry drop outs, result in a signal coverage of approximately 97% for the period investigated here. These gaps are filled with a high order autoregressive model. As with the GOLF signal, the time series gap filling has a negligible effect on the final calculated power spectra and is used here to simplify the temporal filtering.

3.1. Modeling the GOLF signal

The observed GOLF signal is estimated here by using MDI LOI-proxy velocity images along with the GOLF velocity response functions discussed in Sect. 2.1. Following from Eq. (1) the simulated GOLF velocity signal, hereafter referred to as GOLF_sim, can be expressed as

$$\delta v_{\rm sim} = W_0 \int_{disc} S^-_{v,b}\, \delta v_{\rm MDI}\, dA, \qquad (4)$$

where $S^-_{v,b}$ is the sensitivity function for the Na D blue wings with the `$-$´ magnetic modulation, W_0 is defined by Eq. (2) and $\delta v_{\rm MDI}$ is MDI LOI-proxy velocity data. Here we have chosen the negative magnetic modulation. The modulation choice is arbitrary since the signal difference between the sensitivity functions is negligible in terms of the comparison presented here.

The GOLF velocity response function varies spatially across the solar disc depending on the orbital velocity and the observed inclination angle of the solar polar axis, B_0. The individual velocity response functions are interpolated between calculated daily response functions. The daily velocity response functions are created using the average offset velocity and B_0 for each day. All the spatial masking is done in the LOI-proxy bin frame. So, for example, the GOLF velocity sensitivity functions are calculated at a pixel resolution of a 128×128 array and then rebinned using the LOI-proxy mask. An example of a velocity sensitivity function binned using the MDI LOI-proxy mask is shown in Fig. 1.

3.2. Additional spatial masks

In addition to the velocity response functions used to create the GOLF_sim signal, three other spatial masks are applied to the MDI LOI-proxy velocity images for comparison. A particular type of masking, referred to as `zero-sum´, greatly decreases the instrumental background noise in both MDI velocity and intensity data (Scherrer 1997). A zero-sum mask is any mask that has a full-disk integrated value of zero. The effect of the zero-sum masking is quite noticeable and is discussed in more detail in Sect. 4.1.

Besides GOLF_sim, three additional masked signals are used in the comparison: `north-south´, `central region´ and `central zero-sum´. The north-south mask is divided at the image north and south mid-line into two equal parts with equal weight but opposite sign. The central region mask is defined by Gaussian weights centered on the image disc center. The Gaussian is defined such that the 1/e drop-off is at the image radius defining the inner 10% of the image area. The central zero-sum mask

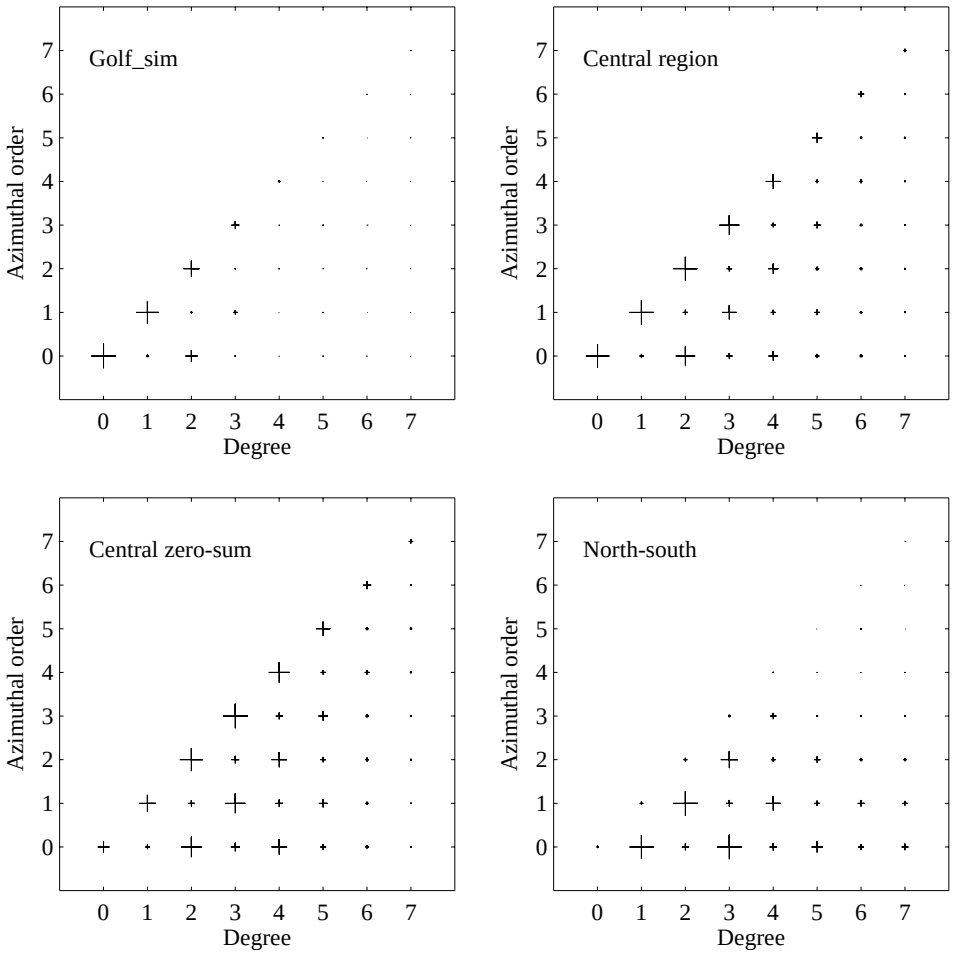

Fig. 3. Comparison of the acoustic mode sensitivity between the four spatial masks used with the MDI full-disk Doppler data as a function of degree ($l \leq 7$) and the azimuthal order ($0 \leq m \leq 7$). The sensitivity maps are for GOLF_sim (*upper left*), central region (*upper right*), and central zero-sum (*lower left*) and north-south (*lower right*). The estimated mode sensitivity map for the LOI-proxy signal (not shown) is very similar to GOLF_sim. The amplitudes of each map are normalized by the maximum. The size of the `+´ symbol is proportional to the sensitivity. These maps are for an average offset velocity of 1050 m/s and B_0 of 7 degrees. Note that the north-south mask predominately selects the $l + m$ odd modes.

is the same as the central region mask except it has a mean of zero. The `raw´ integrated full-disk LOI-proxy velocity signal is referred to hereafter as `LOI-proxy´.

Since each spatial mask has a different response to the observed solar surface velocity field, particular masks are more optimal for various l and m multiplets relative to other masks (e.g. Christensen-Dalsgaard 1984; Kosovichev 1986; Appourchaux & Andersen 1989). Consequently, the measured signal-to-background ratio for a given mode is expected to be dependent on the spatial mask used. Following Christensen-Dalsgaard (1984, 1989), the acoustic mode sensitivity is estimated as a function of degree l and the azimuthal order m for the four spatial masks used in this investigation (see Fig. 3). The numerical details for this calculation are fully described in Henney (1999). In Fig. 3, notice that the central zero-sum is more sensitive to $l = 3, 4, 5$ modes than the other spatially masked signals. In addition, note that the north-south spatial mask is sensitive to the $l + m$ odd modes, whereas the other masks are sensitive to the $l + m$ even modes. The sensitivity of the GOLF_sim mask to the $l + m$ odd modes is a result of the non-homogeneous response of the GOLF instrument over the solar disc (see Fig. 1). Furthermore, the temporal variation of B_0 breaks the full-disk symmetry response of the central and north-south masks. This effect produces an increased sensitivity of the central masks and the north-south mask to the $l + m$ odd and $l + m$ even modes respectively.

3.3. Power spectra fitting

The signal-to-background ratio for low degree ($l \leq 3$) and low frequency ($< 2000\,\mu$Hz) acoustic modes observed in the GOLF and the MDI velocity signals are compared in the following section. The individual mode parameters from the observed power spectra are fit following Anderson et al. (1990) by using maximum likelihood estimator where the model, $\mathrm{M}(\nu)$, is defined as

$$\mathrm{M}(\nu) = \sum_{m=-l}^{l,2} \frac{A_{|m|} w^2}{w^2 + (\nu_0 - \nu + m\, s)^2} \; + \; c. \qquad (5)$$

The mode multiplet amplitude, half-width, frequency and the local background power are represented by $A_{|m|}$, w, ν and c respectively. In addition, the central frequency for each mode and the amount of rotational splitting is represented by ν_0 and s respectively.

The error associated to each parameter is estimated from the width of the corresponding distribution obtained by a Monte-Carlo simulation. For each individual multiplet we use the value of the parameters estimated from the fit to generate a set of 500

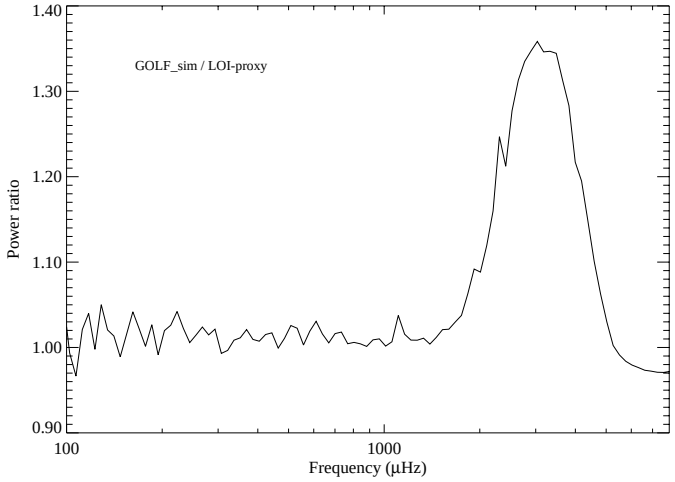

Fig. 4. Ratio of the velocity power spectra of GOLF_sim relative to LOI-proxy for a 759 day period: May 25, 1996 through June 22, 1998. The power spectra are averaged for 100 bins evenly spaced in log frequency over the range shown above.

artificial spectra according to the technique described by Anderson et al. (1990). This approach produces a probability distribution function for each parameter from which the error can be estimated. We have verified that the width of the distributions is in excellent agreement with the mean values of the internal error estimates.

4. Results and discussion

The GOLF signal and the MDI LOI-proxy velocity signals with and without spatial masking are compared in the following subsections. The comparison is for a continuous sequence of 759 days for the period of May 25, 1996 through June 22, 1998.

4.1. Power spectra comparison

The power spectra of LOI-proxy and GOLF_sim are very similar. The ratio of the two power spectra are shown in Fig. 4, which exhibits an enhancement of the GOLF_sim signal in the 5-minute band. The power spectra for the GOLF and the spatially masked MDI velocity signals are shown in Fig. 5. For the LOI-proxy, north-south and GOLF_sim signals the power in the 5-minute band is below that observed from GOLF. This power difference is expected since velocity scales with atmospheric height and GOLF observes at an altitude above MDI. The MDI central region signals have additional power from higher degree modes, which accounts for the increased power observed from these signals compared to GOLF in the 5-minute band.

For frequencies above the 5-minute band, the differences between the power spectra are quite noticeable. Between the MDI signals, the overall reduction in instrumental noise for the zero-sum masked signals is readily evident in the north-south and the central zero-sum signals shown in Fig. 5. The source of this instrumental full-disk signal is believed to be due to variations in the shutter effective open duration when a major frame pulse occurs during exposure (Scherrer 1997).

In addition to the reduction of the shutter background noise, the zero-sum masked signals have nearly no contribution from the $l = 0$ modes. The power spectra of the north-south signal is further reduced relative to the other signals since the spatial masking filters out the sectoral modes.

The difference between the GOLF and MDI power spectra for frequencies below the 5-minute band, near 1500 μHz, is also quite noticeable in Fig. 5. The MDI zero-sum masked signals have the lowest background power in this region. The MDI LOI-proxy and GOLF_sim power is above the zero-sum signals due to the shutter background noise. The power in the GOLF and central region signals is higher near 1100 μHz which is most likely due to contribution from granulation.

In Fig. 6 the ratio of the power spectra illustrates the differences in the background power as observed by MDI and GOLF. Most of the variation between the MDI signals shown in Fig. 6 is a result of the shutter noise background. The GOLF signal relative to the MDI signals with a zero-sum spatial mask exhibits a broad band excess centered near 1000 μHz ($\sim$16 minutes) and a strong broad band excess centered near 5700 μHz ($\sim$3 minutes). These two power bands in the GOLF signal relative to MDI are similar to the ratio of the GOLF spectra reduced from one-wing data relative to two-wing data during the period when GOLF observed both wings of the Na D lines (e.g. Gabriel et al. 1997 and Henney et al. 1998b). In earlier comparisons between GOLF and MDI velocity power spectra, the 16-minute and 3-minute broad band power difference were reported by Scherrer (1997), García (1997) and Henney et al. (1998b). The substantial difference shown in the power ratio near 5700 μHz in Fig. 6 is most likely the result of intensity-like contributions from chromospheric oscillations (e.g. Noyes 1966). In Fig. 6, the GOLF power spectra bulge centered near 1000 μHz may be the result of velocity and intensity contributions from granulation overshoot (e.g. Harvey et al., 1993). Notice in Fig. 6 that within the frequency band of 1800 to 4000 μHz, the power spectra ratio of GOLF relative to the zero-sum signals along with the central region signal are at a local minimum.

In the frequency range of interest for g-modes, below 500 μHz, the power of the GOLF signal is at least twice the power of the MDI signals, except for the central zero-sum signal. Although the nature of this difference is currently uncertain, it may be produced by a combination of the altitude difference in the solar atmosphere observed by the two instruments and intensity contribution from supergranulation. In addition, the lack of an absolute calibration for the signals investigated in this work may play an important role in this comparison. The closer agreement between GOLF and MDI signal is achieved when the central zero-sum spatial mask is used, in particular at frequencies below 300 μHz. A cross analysis of these two signals may be useful for verification of future g-mode candidates.

4.2. Signal-to-background comparison

A detailed comparison of the GOLF and the MDI power spectra for low degree modes ($l \leq 3$) is shown in Fig. 7. Notice the enhanced signal amplitude for the $l = 3$ acoustic mode between

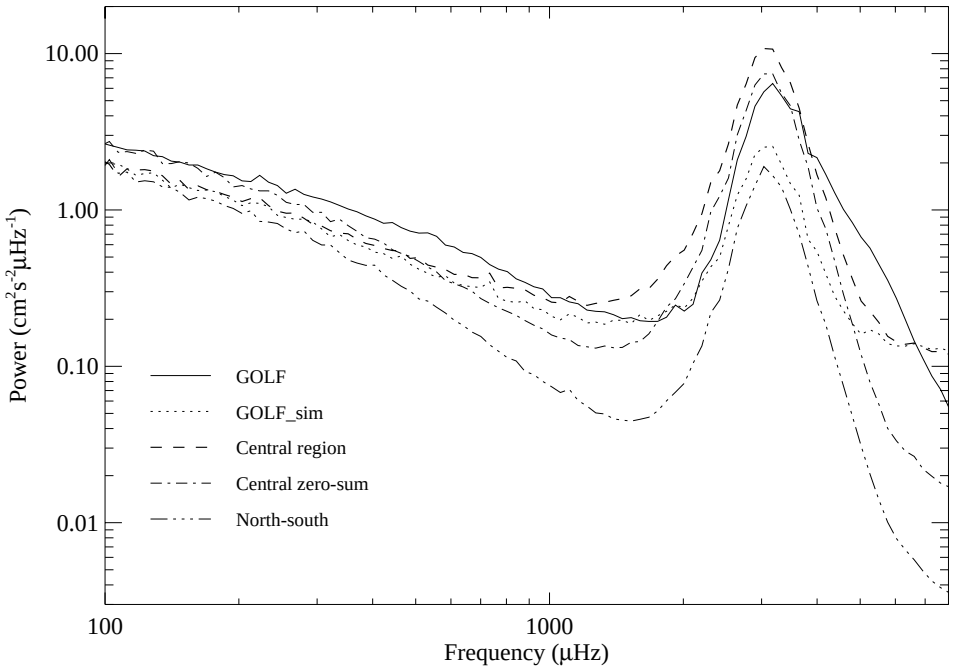

Fig. 5. Comparison of the GOLF power spectra and the MDI LOI-proxy velocity power spectra with and without spatial masking for a 759 day period: May 25, 1996 through June 22, 1998. Each power spectrum is averaged for 100 bins evenly spaced in log frequency over the range shown above.

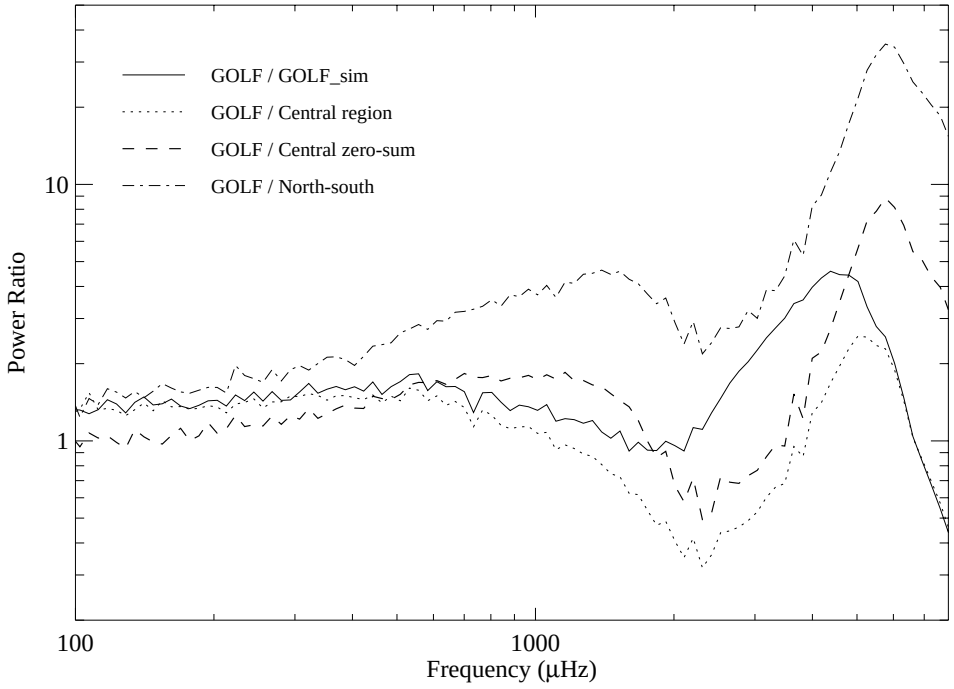

Fig. 6. The log of the power spectra ratio of the GOLF and MDI signals for a 759 day period: May 25, 1996 through June 22, 1998. Each power spectrum is averaged for 100 bins evenly spaced in log frequency over the range shown above.

the GOLF and the MDI north-south and central region masked data in Fig. 7. As a relative measure of merit for each time series, the signal-to-background ratio, S/B, for modes within the frequency range 1200–2100 μHz are compared here. The `signal´ is defined as the sum of the mode multiplet amplitude, $A_{|m|}$, and the background, c, from the fit of the power spectra using Eq. (5). For each power spectrum, except the north-south masked signal, the multiplet pairs for the sectoral modes of degree $l \leq 3$ are compared in Fig. 8. The north-south signal is not compared here since it is primarily comprised of zonal and tesseral modes (see Fig. 7). The S/B results shown in Fig. 8 are obtained from the power spectra fitting procedure described in Sect. 3.3.

For the frequency range and the signals compared in this work, the GOLF signal has the highest S/B for $l = 0$ acoustic modes. Also illustrated in Fig. 8 is that the S/B of the GOLF and central region data are both good for detecting $l = 1$ acoustic modes. For $l \geq 2$ modes, the central region masked signals have the highest S/B values compared to GOLF, LOI-proxy and GOLF_sim. Between the MDI signals, the GOLF_sim S/B is found to be slightly systematically higher than the MDI LOI-proxy signal without spatial masking (see Fig. 8). In addition,

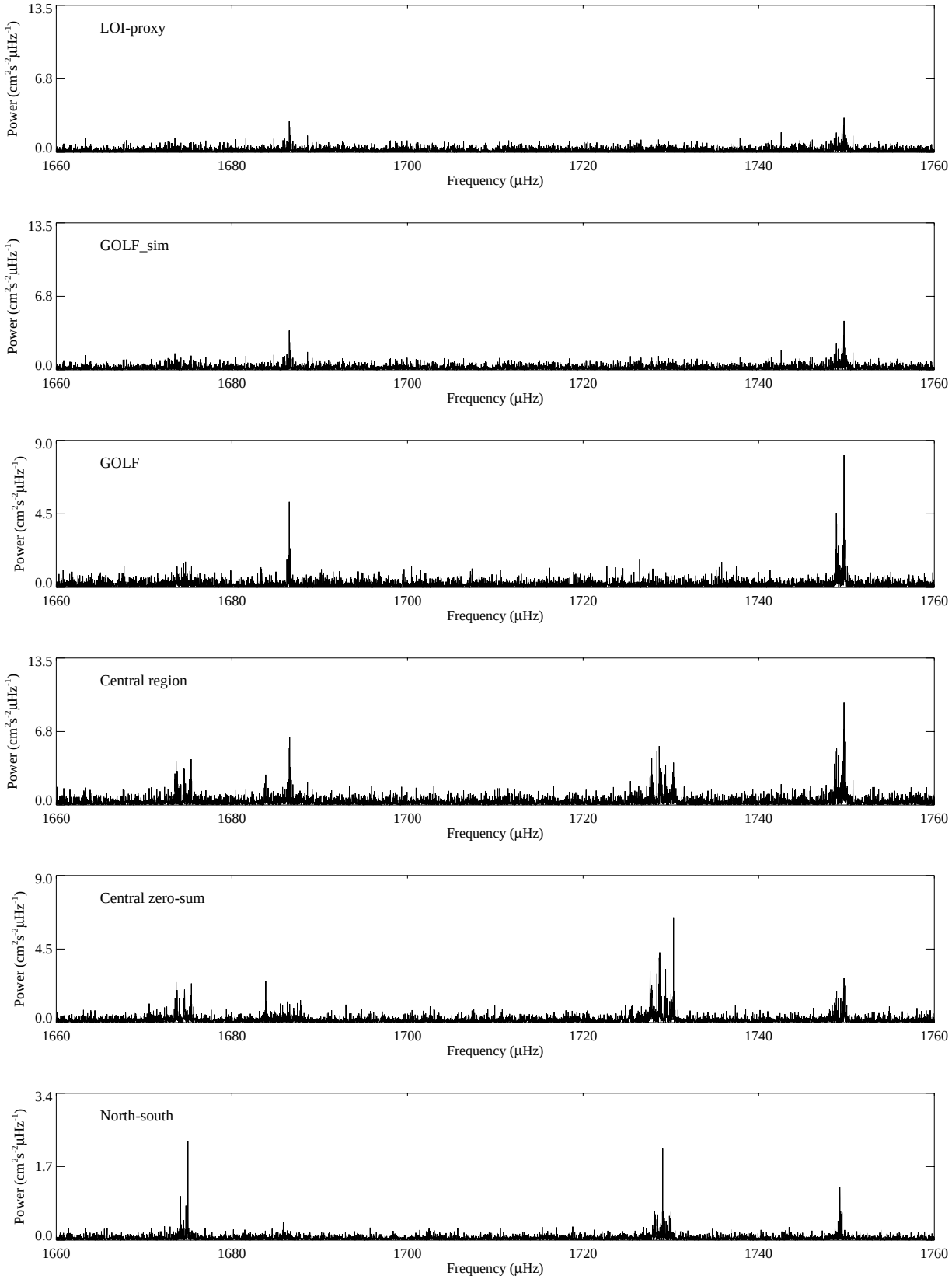

Fig. 7. The GOLF power spectra along with the MDI LOI-proxy velocity power spectra with and without spatial masking for a 759 day period: May 25, 1996 through June 22, 1998. The clearly noticeable acoustic modes in the central region panel, from left to right, are: $l = 2,\ n = 10;\ l = 0,\ n = 11;\ l = 3,\ n = 10$; and $l = 1,\ n = 11$. Note that the north-south signal is predominately comprised of $l + m$ odd modes. In addition, note that a $l = 5$ mode is detectable visible near 1685 μHz in the bottom three panels.

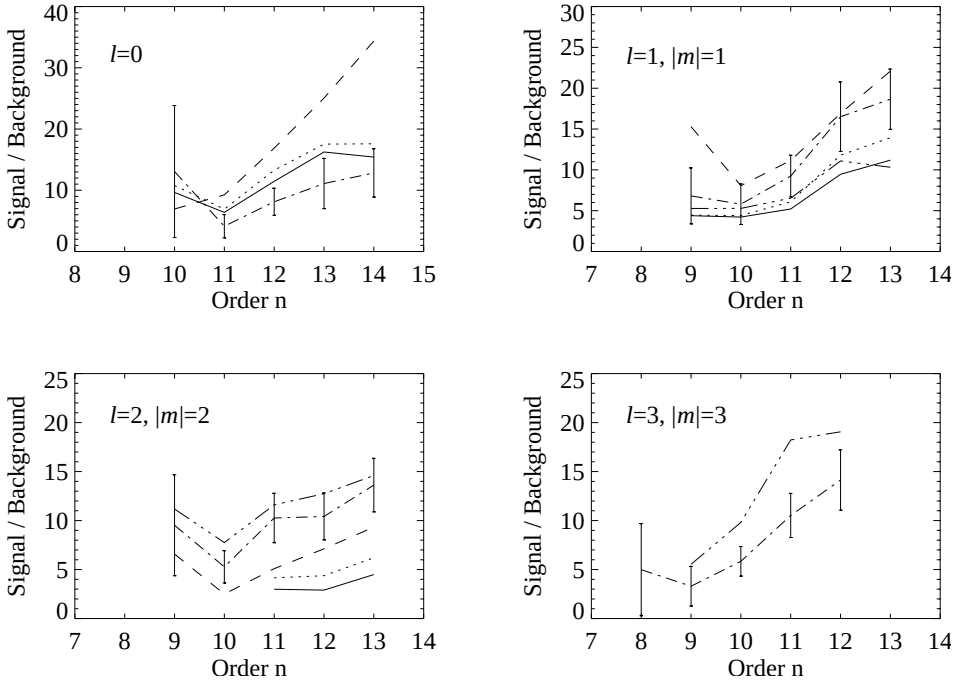

Fig. 8. Comparison of low frequency acoustic mode signal-to-background ratios (S/B) for different MDI masked signals with the GOLF signal. The S/B are compared for the sectoral acoustic modes of $l = 0$ (*top left*), $l = 1$ (*top right*), $l = 2$ (*bottom left*) and $l = 3$ (*bottom right*). The S/B values for LOI-proxy (solid), GOLF_sim (dot), GOLF (dash), central region (dot-dash), and central zero-sum (three dots-dash) are shown. The signal is defined as the mode multiplet amplitude plus the background from the model fit. The error bars are 1σ and are only shown for the central region signal for visual clarity and are representive of the estimated errors for the other signals.

the GOLF_sim signal has the highest S/B on average relative to the other MDI signals compared for the l=0 modes shown in Fig. 8.

The S/B for a given mode may be improved by averaging the GOLF spectra with a corresponding MDI masked spectra. In addition, cross spectral analysis may be useful for the time series with similar signals but different backgrounds due to the different spatial weighting of supergranules. Further S/B improvements may come from future additions to the GOLF-simulated signal which account for active region effects. Intensity fluctuations associated with magnetic activity produce velocity signal amplitudes as large as $\sim$7 m/s with periods on the order of a few days for measurements such as done by GOLF (e.g. Ulrich et al. 1993). To estimate these effects for the observed GOLF signal, the GOLF-simulated signal will incorporate the MDI line-depth images, as a magnetic proxy, along with MDI line-continuum images (e.g. Ulrich et al. 1999). In this way we hope to model and understand the low frequency background power in the GOLF signal associated with magnetic activity. Ultimately we want to match frequencies of agreed signals between the two instruments regardless of predicted mode frequencies.

5. Conclusion

We find that signals from both MDI and GOLF are beneficial for detecting low degree ($l \leq 3$) and low frequency ($< 2000\,\mu$Hz) acoustic modes. For the frequency range and the signals compared in this paper, the GOLF signal has the highest S/B for $l = 0$ acoustic modes. The S/B of the GOLF and MDI central region masked signals is good for detecting $l = 1$ acoustic modes. For $l \geq 2$ modes, the central region masked signals have the highest S/B of the power spectra compared in this paper. In addition, the S/B of the preliminary GOLF-simulated signal, GOLF_sim, is found to be more similar to the GOLF signal than the MDI LOI-proxy signal without spatial masking for the modes investigated here. Future improvements of the GOLF_sim signal and the use of optimal mask for selected modes may be helpful in future cross-analysis between GOLF and MDI in the search for new low frequency modes.

Acknowledgements. We thank the referee, Thierry Appourchaux, for his prompt and careful review of this paper, along with his useful suggestions. In addition, we are grateful to Alexander Kosovichev for his helpful comments on an earlier draft of this paper. This research is supported by a NASA subcontract to UCLA through Stanford University. The GOLF instrument was constructed by a consortium of French and Spanish institutes, supported by a large number of scientific investigators from many counties. SOHO is a mission of international cooperation between ESA and NASA.

References

Anderson E.R., Duvall T.L., Jefferies S.M., 1990, ApJ 364, 699
Appourchaux T., Andersen B.N., 1989, Solar Physics 128, 91
Appourchaux T., Andersen B.N., Fröhlich C., et al., 1997, Solar Physics 170, 27
Bertello L., Henney C.J., Ulrich R.K., et al., 1998, In: Korzennik S., Wilson A. (eds.) Proceedings of the SOHO 6/GONG 98 Workshop, Structure and Dynamics of the Interior of the Sun and Sun-like Stars. ESA Publications, Noordwijk, ESA SP-418, p. 115
Christensen-Dalsgaard J., 1984, In: Ulrich R.K., Harvey J., Rhodes E.J., Toomre J. (eds.) Solar Seismology from Space. NASA, JPL Publ. 84-84, p. 219
Christensen-Dalsgaard J., 1989, MNRAS 239, 977
Duvall T.L. Jr., Kosovichev A.G., Scherrer P.H., et al., 1997, Solar Physics 170, 63
Fröhlich C., Romero J., Roth H., et al., 1995, Solar Physics 162, 101
Fröhlich C., Andersen B.N., Appourchaux T., et al., 1997, Solar Physics 170, 1

Gabriel A.H., Grec G., Charra J., et al., 1995, Solar Physics 162, 61
Gabriel A.H., Charra J., Grec G., et al., 1997, Solar Physics 175, 207
García R.A., 1997, GONG/SOI/VIRGO Workshop on Resonant Mode Identification, 3–6 December, 1997, Stanford, California
Harvey J.W., Duvall T.L. Jr., Jefferies S.M., Pomerantz M.A., 1993, In: Brown T.M. (ed.) Proceedings from GONG 1992, Seismic Investigation of the Sun and Stars. ASP Conf. Ser. 42, p. 111
Henney C.J., 1999, Ph.D. dissertation, University of California, Los Angeles
Henney C.J., Ulrich R.K., Bertello L., et al., 1998a, In: Korzennik S., Wilson A. (eds.) Proceedings of the SOHO 6/GONG 98 Workshop, Structure and Dynamics of the Interior of the Sun and Sun-like Stars. ESA Publications, Noordwijk, ESA SP-418, p. 213
Henney C.J., Bertello L., Ulrich R.K., et al., 1998b, In: Korzennik S., Wilson A. (eds.) Proceedings of the SOHO 6/GONG 98 Workshop, Structure and Dynamics of the Interior of the Sun and Sun-like Stars. ESA Publications, Noordwijk, ESA SP-418, p. 219
Hoeksema J.T., Bush R.I, Mathur D., Morrison M., Scherrer P.H., 1998, In: Provost J., Schmider F.-X. (eds.) Sounding Solar and Stellar Interiors. IAU Symposium 181, Poster Volume, p. 31
Kosovichev A.G., 1986, Izv. Krymsk. Astrofiz. Obs. 75, 22
Kosovichev A.G., Schou J., Scherrer P.H., et al., 1997, Solar Physics 170, 43
Noyes R.W., 1966, In: Thomas R.N. (ed.) Aerodynamic Phenomena in Stellar Atmospheres. IAU Symposium 28, p. 293
Pallé P.L., Régulo C., Roca Cortés T., et al., 1999, A&A 341, 625
Scherrer P.H., 1997, GONG/SOI/VIRGO Workshop on Resonant Mode Identification, 3–6 December, 1997, Stanford, California
Scherrer P.H., Bogart R.S., Bush R.I., et al., 1995, Solar Physics 162, 129
Toutain T., Appourchaux T., Baudin F., et al., 1997, Solar Physics 175, 311
Turck-Chièze S., Basu S., Brun A.S., et al., 1997, Solar Physics 175, 247
Ulrich R.K., Henney C.J., Schimpf S., et al., 1993, A&A 280, 268
Ulrich R.K., García R.A., Robillot J.-M., et al., 1998, In: Korzennik S., Wilson A. (eds.) Proceedings of the SOHO 6/GONG 98 Workshop, Structure and Dynamics of the Interior of the Sun and Sun-like Stars. ESA Publications, Noordwijk, ESA SP-418, p. 353
Ulrich R.K., Boumier P., Robillot J.-M., et al., 1999, A&A, submitted